FULL PAPER
THE ANALYST
www.rsc.org/analyst

A glucose dehydrogenase biosensor as an additional signal amplification step in an enzyme-flow immunoassay

Catalin Nistor,[a] Andreas Rose,[b] Ulla Wollenberger,[b] Dorothea Pfeiffer[c] and Jenny Emnéus*[a]

[a] *Department of Analytical Chemistry, Lund University, P.O. Box 124, S-221 00 Lund, Sweden. E-mail: jenny.emneus@analykem.lu.se; Fax: +46 46 222 45 44; Tel: +46-46-2224820*
[b] *Department of Analytical Biochemistry, University of Potsdam, D 14476 Golm, Karl-Liebknecht-Str. 24-25, Germany*
[c] *Biosensor Technology GmbH (BST), Berlin, Germany*

Received 9th April 2002, Accepted 11th June 2002
First published as an Advance Article on the web 16th July 2002

Both the antibody affinity and the detectability of the label are essential in deciding the final characteristics of a heterogeneous immunoassay. This paper describes an approach to obtain a supplementary enhancement of the signal generated by using an enzyme label, *e.g.*, by including the product of the enzymatic reaction in an additional amplification cycle during the detection step performed with an amperometric biosensor based on glucose dehydrogenase (GDH). An immunoassay format with a labelled analyte derivative that competes with the analyte present in the sample for a limited amount of antibody binding sites was employed. The β-galactosidase label hydrolyses the substrate aminophenyl-β-galactopyranoside, and the generated aminophenol enters then into a bioelectrocatalytic amplification cycle at the GDH biosensor. The principle was applied for determination of 4-nitrophenol, with the best minimal concentration of 1.5 μM and a midpoint of the calibration of 24 μM. The potentials and limitations of such a system are discussed.

Introduction

Short analysis time, portability and high sensitivity obtained with minimum costs for equipment and reagents are only a few requirements for modern methods to be used in environmental and clinical analysis. Immunoassays with electrochemical detection represent good alternatives in this sense. They have gained more and more importance in recent years because of their inherent sensitivity, potential for miniaturisation and multianalyte identification, as well as the possibility of measurement with minimal interferences even in coloured and turbid samples.[1]

Because of the inherent amplification, the use of enzymes as labels is currently the most frequently adopted detection alternative in heterogeneous and homogeneous immunoassays. Alkaline phosphatase (ALP), using aminophenylphosphate (APP) as the substrate and the oxidative amperometric detection of the generated aminophenol (AP) has been the most extensively employed electrochemical immunoassay principle.[1–7] However, peroxidase[8–13] and β-galactosidase (β-Gal)[5,14–16] have also often been used as labels in electrochemical immunoassays.

Recently, the improvement of tracer detectability has been demonstrated by using an additional amplification step at the detection level, *e.g.*, combination of the immunoassay with detection of the product generated by the enzyme label at an electrochemical biosensor. Thus, the reaction catalysed by ALP employed as label in an immunoassay for thyrotropin was performed on a peroxidase-based biosensor,[17] using 5-bromo-4-chloro-3-indolylphosphate as ALP substrate. ALP was also used as an enzyme label in combination with a bienzymatic biosensor consisting of tyrosinase (Tyr) and pyrroquinoline quinone (PQQ)-dependent glucose dehydrogenase (GDH). The two enzymes were co-immobilised on the active surface of a Clark-type electrode and employed as detectors either in a competitive,[18] or non-competitive[19] immunoassay format. The enzyme label initially converts phenylphosphate (PP) into phenol, which is further recognised by Tyr and transformed sequentially into *o*-catechol and *o*-quinone. The latter is a co-substrate for the enzyme GDH, which converts the quinone back to catechol in the presence of its main substrate, glucose. An amplification cycle is thus created, and the whole process can be sensitively quantified by monitoring the oxygen consumption in the reaction catalysed by Tyr. In a bioelectrocatalytic approach, applied for determination of the drug digoxin, Tyr was immobilised on a carbon paste electrode, and the regeneration of the quinone generated by Tyr was electrochemically reduced back to catechol at −50 mV *vs.* Ag/AgCl,[20] so that an additional amplification of the original current could be measured.

In a different configuration, a β-Gal labelled analyte was used in a competitive immunoassay for determination of atrazine.[16] The enzyme label converts the substrate aminophenylgalactopyranoside (APG) to galactose and AP, which was electrochemically oxidised to iminoquinone (IQ) at +250 mV *vs.* Ag/AgCl. The enzyme immobilised on the electrode surface, cellobiose dehydrogenase (CDH), uses IQ as the co-substrate in the presence of cellobiose, and transforms it back to AP, generating a signal enhancement. Even though this improvement in detection was only 3–5 times[21] when employing a CDH biosensor instead of a bare graphite electrode, the system allowed determination of atrazine in the ng L^{-1} range. Additionally the biosensor detection led to a considerable reduction of matrix interferences, if compared to spectrophotometric detection, when surface water samples were analysed.[16]

A similar detection principle as the one described above was used in this paper, employing a β-Gal-labelled analyte derivative in an enzyme flow immunoassay (EFIA) format for determination of 4-nitrophenol (4-NP), in combination with an amperometric biosensor based on PQQ-dependent GDH. This biosensor was shown to be much more sensitive for detection of

 DOI: 10.1039/b203452b

4-AP than the CDH-based electrode,[22] (see also below), and it also led to a lower detection limit for β-Gal in comparison to a plain electrode or a CDH-based biosensor.[21] As will be shown later in this paper, the assay principle proved to work, however certain technical aspects limited the improvement in assay sensitivity, and these will also be discussed.

Experimental

Chemicals and tracer synthesis

A 4-NP derivative (*S*-(hydroxyl-5-nitrobenzyl)propionic acid, HOM), with the structure given in Fig. 1, kindly provided by Dr. M.-P. Marco, IIQAB-CSIC, Barcelona, Spain, and β-galactosidase (β-Gal, enzyme immunoassay grade from *E. coli*, Roche Biochemicals) were employed for tracer synthesis according to the following steps.

(1) The carboxy group of the HOM derivative was pre-activated by reaction of 15 μmol of HOM (3.86 mg) with activation reagents. Two different activation procedures were used:

Activation procedure I. 75 μmol (8.62 mg) *N*-hydroxysuccinimide (NHS, Cat. No. H-7377, Sigma Chemical Co., St. Louis, MO, USA) and 150 μmol dicyclohexylcarbodiimide (Cat. No. 36650, Fluka Chemie AG, Buchs, Switzerland) were dissolved in 50 μl dry dimethylformamide (DMF, Cat. No. 7027, Baker, Germany) and added to 15 μmol HOM in 50 μl dry DMF. The mixture was stirred for 1 h at room temperature and the resulting white precipitate of dicyclohexyl urea was removed by centrifugation for 10 min at 10000 rpm, while the supernatant was used for further conjugation.

Activation procedure II. 50 μl dry DMF, containing 15 μmol (5.48 mg) 2-(5-norbornene-2,3-dicarboximido)-1,1,3,3-tetramethyluronium tetrafluoroborate (TNTU, Cat. No. LA10120//01-62-0024, Calbiochem-Novabiochem, Länfelfingen, Germany) and 15 μmol *N*-methylmorpholin (NMM, Cat. No. 67869, Fluka) were added under stirring to 50 μl dry DMF, containing 15 μmol HOM and the mixture was stirred for an additional 15 min at room temperature. A clear solution containing the activated HOM was obtained, and used for further conjugation without additional purification.

(2) The two pre-activated HOM derivatives were coupled to β-Gal according to the following procedure: to obtain tracers with an initial molar ratio of 1000 mol HOM to 1 mol of β-Gal, 10 μl (1.5 μmol) each of the NHS and TNTU activated HOM conjugates were added drop-wise and under stirring to 4.05 mg β-Gal (1.5 nmol) dissolved in 200 μl 0.1 M carbonate buffer pH 8.25.

For preparation of the tracers with initial molar ratios of 100 : 1, 10 : 1 and 1 : 1 HOM to β-Gal the activated HOM solutions were diluted to 1 : 9, 1 : 99 and 1 : 999 (v/v), respectively, with dry DMF. Then, 10 μl of each resulting solution were added drop-wise to 1.5 nmol β-Gal. All the coupling reactions were allowed to proceed overnight at 4 °C.

(3) Purification of the tracers from the unconjugated HOM derivative was performed by dialysis (Slide-A-Lyzer®, 500 μl dialysis cassettes, Cat. No. 66415, molecular weight cut-off 10 KDa, Pierce Chemical Co., Rockford IL, USA) against 2 l of 0.1 M tris(hydroxymethyl)aminomethane buffer (TRIS, Cat. No 93352, Fluka), pH 7.5, containing 1 mM $MgCl_2$ (Merck, Darmstadt, Germany).

Instrumentation and methods

Enzyme flow immunoassay (EFIA)

In principle, two types of experiment were performed for each of the synthesised tracers. (see Fig. 1) *Optimisation of the antibody concentration*, *i.e.*, generation of an antibody dilution curve was carried out by incubation of different concentrations of antibody (Ab) with a minimal and constant concentration of tracer (Ag*), which gave a signal of 120–150 nA at 100% bound fraction, corresponding to a signal-to-noise ratio of 160–200. After incubation, the mixture was introduced into the flow system and the amount of trapped Ag* was monitored as described below. The *antigen calibration curve* was accomplished similarly, except that the reaction mixture consisted of different concentrations of analyte mixed with the optimised and constant concentrations of tracer and antibody determined above.

After 15 min competitive off-line incubation of the analyte (4-NP, Cat. No. 73560, Fluka), β-Gal tracer and antibody (As36, polyclonal from rabbit, kindly provided by Dr. M.-P. Marco), the mixture was injected into the flow system *via* a 50 μl injection loop connected to a manually-driven six port injection valve (Rheodyne, Berkley, CA, USA). The sample was transported by a peristaltic pump (Minipuls 3, Gilson, Villiers-le-Bel, France), continuously pumping a carrier buffer containing 20 mM *N*-(2-hydroxyethyl)-piperazine-*N*′-(2-ethanesulfonic) acid (HEPES, Cat. No. H-3375, Sigma) at pH 7.5, containing 20 mM KCl (Merck), 1 mM $CaCl_2$ (Merck), 1 mM $MgCl_2$ (Merck), 10 mM glucose (Merck), 0.01% (v/v) polyoxyethylenesorbitan monolaureate (Tween 20, Cat. No. P-1379,

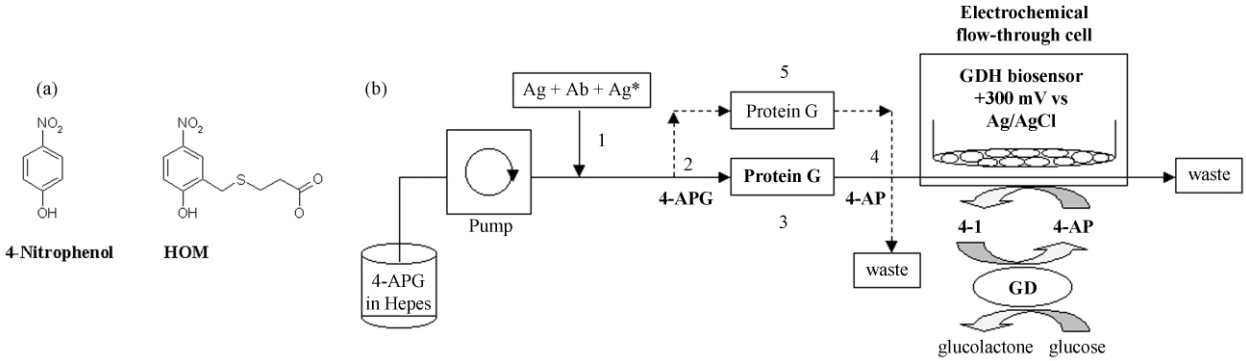

Fig. 1 (a) Structures of the analyte (4-nitrophenol) and of the hapten derivative used for tracer synthesis; (b) schematic representation of the flow-injection system and the working mechanism of the GDH biosensor: (1) injection of the sample mixture containing the analyte tracer (a β-Gal conjugate of HOM) and antibody at equilibrium; (2) trapping the antibody-complexed analyte and tracer on the protein G column and removal of the free fractions; (3) the carrier flow through the protein G column is stopped for 2.5 min; (4) the carrier flow is re-started and the 4-AP produced is measured by the GDH biosensor; (5) the protein G column is disconnected and regenerated.

Sigma), and 50 μM 4-aminophenyl-β-D-galactopyranoside (4-APG, Cat. No. A-9545, Sigma), at a flow rate of 0.5 ml min^{-1}. The unbound analyte and tracer were separated from the antibody–antigen and antibody–tracer complexes formed by trapping the immuno-complexes in a column (0.2 × 2.5 cm) filled with protein G immobilised on sepharose (HiTrap®, Cat. No. 17-0404-03, Amersham Biosciences, Uppsala, Sweden). This column was placed instead of an injection loop in a second six-port injection valve (Rheodyne), allowing it to be switched in to or out of the carrier flow for regeneration between runs with 0.1 M glycine buffer (Cat. No. G-7126, Sigma), adjusted to pH 2.5 with HCl.

After injection of the sample mixture, the protein G column was washed for 2 min with carrier buffer containing the enzyme substrate, then the flow through the protein G column was stopped for 5 min. During this time, the enzyme tracer trapped inside the column converted 4-APG to 4-aminophenol (4-AP). When the flow was re-started, the formed 4-AP was eluted by the carrier flow and electrochemically detected downstream on the screen-printed biosensor.

PQQ-dependent GDH (EC 1.199.17, from recombinant *E. coli*, original gene from *Acinetobacter calcoaceticus*, gift of Roche, Indianapolis, USA) and screen-printed electrodes from BST (BioSensor Technologie GmbH, Berlin, Germany) were used for preparation of the biosensors, as previously described.[22] The electrochemical measurements were performed in an in-house built two-electrode flow cell.[22] 4-AP generated in the reaction catalysed by β-Gal was firstly oxidised to the corresponding IQ at the GDH working electrode, poised at a potential of +300 mV *vs.* Ag/AgCl. The resultant IQ was reduced back to 4-AP by GDH forming the oxidised form of the enzyme (GDH_{ox}). Subsequently, the active reduced enzymatic form (GDH_{red}) was regenerated by oxidation of the glucose present in excess in the carrier buffer. Since both 4-AP and the GDH_{ox} were reformed, a new bioelectrocatalytic cycle could be initiated, thus resulting in an overall amplification of the 4-AP oxidation current. The GDH biosensor was calibrated with 4-AP solutions of concentrations between 10 and 1000 nM prior to each EFIA experiment.

When not in use the screen-printed sensors were kept at 4 °C in a solution of 100 nM PQQ, kindly provided by Roche, Indianapolis, USA. The generated current was registered by a recorder (Kipp&Zonen, Delft, The Netherlands).

Microtiter plate enzyme-linked immunosorbent assay (ELISA). A direct competitive ELISA was performed by first coating microtiter plates (Nunc Maxisorp, Nunc. Co., Roskilde, Denmark) with 100 μl $well^{-1}$, containing 10 μg ml^{-1} As36 in 0.1 M carbonate buffer at pH 9.6. The adsorption was allowed to take place overnight at 4 °C. The excess of unbound As36 was repeatedly washed away with phosphate buffered saline (PBST) at pH 7.2 containing 40 mM Na_2HPO_4/KH_2PO_4, 137 mM NaCl, 3 mM KCl (all from Merck), and 0.05% (v/v) Tween 20. The free unspecific binding sites were blocked by addition of 100 μl $well^{-1}$, containing 0.5% bovine serum albumin (BSA, Sigma) in 0.1 M carbonate buffer at pH 9.6, and incubated at room temperature for 2 h. The excess of BSA was removed by washing the plate with PBST. The competition step was accomplished by addition of different concentrations of analyte (4-NP) and fixed concentrations of tracers dissolved in 50 mM phosphate buffer at pH 7.0, and incubating for 60 min. After washing away the unbound reagents with PBST, 100 μl $well^{-1}$ of 4.15 mM of the β-Gal substrate 4-nitrophenyl-β-D-galactopyranoside (4-NPG, Cat. No. N-0877, Sigma) in 0.1 M phosphate buffer containing 0.1 M NaCl and 1 mM $MgCl_2$ at pH 7.5, was added and incubated with the bound tracer fraction. The liberated 4-NP was monitored after 20 h at 405 nm using a SLT340 ATTC (SLT Lab Instruments, Crailsheim, Germany) microtiter plate reader.

Activity measurement and tracer characterisation

Activity measurements were performed on a Beckman 640 spectrophotometer (Beckman Instruments Inc., Fullerton, CA, USA). Batch activity measurements were carried out spectrophotometrically at 405 nm by monitoring the 4-NP released by β-Gal hydrolysis of 4-NPG, at the conditions specified by the enzyme supplier (Roche Biochemicals). The β-Gal activity measurements were also performed in the flow system, by injection of 50 μM 4-APG in HEPES buffer at pH 7.5, containing 20 mM KCl, 1 mM $CaCl_2$, 1 mM $MgCl_2$, 10 mM glucose and 0.01% Tween.[20] The peak height due to the bioelectrocatalytic current generated for 4-AP oxidation on the GDH electrode was registered, and the activity expressed as μmol 4-AP produced min^{-1} ml^{-1}.

The tracers were characterised in terms of a HOM to β-Gal molar ratio by estimation of the protein concentration using the method described by Bradford.[23] The HOM concentration was estimated by measuring the specific absorbance at 420 nm (ε_{420} = 1.18 cm^2 μmol^{-1}).

The apparent affinity for the antibody–tracer (K_{aff}^{app*}) and antibody–analyte (K_{aff}^{app}) interactions were graphically estimated using a theoretical model based on the law of mass action.[24,25] These are not 'true' affinity constants, but characterise the whole assay system, including the analyte–antibody–tracer interactions and the processes that took place in the flow system, and were mainly used for comparison purposes.

Results and discussion

GDH biosensor

Fig. 2 shows the comparison of direct and amplified detection of 4-AP on a plain Pt electrode and a GDH screen-printed electrode, respectively. It is evident that there is a considerable amplification of the signal when the GDH biosensor is used. The same types of GDH electrodes were previously used for analysis of various phenolic compounds.[22] 4-IQ proved to be one of the best co-substrates for GDH, with a limit of detection (LOD) of 0.72 ± 0.04 nM, a slope of 90 ± 4 nA μmol^{-1}, and a dynamic range of 1–500 nM. This can be compared to the response of direct oxidation of 4-AP on the plain Pt electrode, leading to an LOD of 56 ± 3 nM and a slope sensitivity of 1.01 ± 0.06 nA μmol^{-1}. The stability of the GDH sensor was impressive, giving the possibility of every day use without any major changes in response for about 50 days, using 100 nM dopamine as the reference analyte. All these characteristics

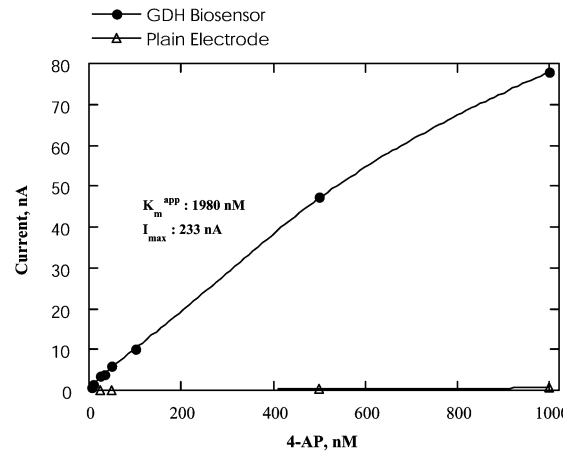

Fig. 2 Calibration for 4-AP at the GDH biosensor. Carrier buffer: 20 mM HEPES, pH 7.5, containing 20 mM KCl, 1 mM $CaCl_2$ and 10 mM glucose; flow rate: 0.5 ml min^{-1}; applied potential: +400 mV *vs.* Ag/AgCl reference/counter-electrode.

make the GDH sensor very suitable as a detector for β-Gal activity in a flow immunoassay.

Characterisation of tracers

Fig. 3 shows the relative specific activity of the β-Gal tracers, as well as the calculated HOM : β-Gal molar ratio *vs.* the initial HOM : β-Gal molar ratio, for both procedures used for tracer synthesis (*i.e.*, I and II, see section 'Experimental', Chemicals and tracer synthesis). The decrease in the activity with the number of HOM molecules covalently bound to one enzyme molecule may be due to unfavourable conformational changes that take place when more nitrophenol groups are linked to the protein structure. On the other hand, the higher the density of hapten derivatives on the enzyme, the higher the affinity of the antibody for the tracer is expected and also experimentally found, as seen in Table 1. The latter leads to lower antibody consumption, which is a factor that has to be taken into consideration in assay development when production of the antibodies is costly. In addition, depending on what the limitations are for a particular application, *i.e.*, low LOD, broad dynamic range, *etc.*, different tracers might prove to be useful for a particular need. The difference in activity of the tracers obtained by the two different activation procedures (*i.e.*, I and II) could be due to a higher biocompatibility of activation procedure II (the TNTU-activated HOM), a procedure that generally leads to a lower coupling yield, *i.e.*, a lower HOM : β-Gal molar ratio, as seen in Fig. 3.

The same trend in the specific activity of the tracers was observed when the measurements were performed in the flow system, using the amperometric biosensor as the detector (results not shown).

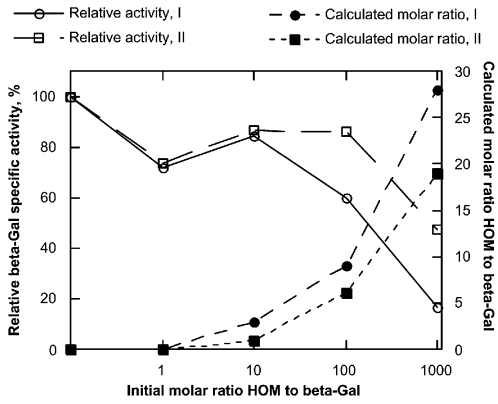

Fig. 3 Relative β-Gal specific activity in relation to the number of HOM molecules conjugated to one protein molecule. Open symbols present the specific activity of the tracers in relation to the activity of β-Gal used as reference. Closed symbols show the calculated molar ratio between the hapten and enzyme label for each tracer.

Table 1 The effect of the HOM : β-Gal molar ratio on the apparent affinity constants for the tracer and analyte

AP[a]	HOM : β-Gal, initial molar ratio	K^*_{app}[b]/μM^{-1}	K^*_{app}/K_{app}[c]
I	10 : 1	10.9	180
I	100 : 1	25.0	407
I	1000 : 1	35.6	585
II	10 : 1	15.2	254
II	100 : 1	30.6	528
II	1000 : 1	41.4	704

[a] AP, activation procedure. [b] K^*_{app}, apparent affinity for the antibody tracer interaction. [c] K^*_{app}/K_{app}, ratio between the apparent affinity for the tracer and analyte. K_{app} for the analyte is basically constant (*i.e.*, 0.06 μM^{-1}) for all cases.

EFIA

β-Gal detection. When the 4-APG was introduced into the flow (at point A, Fig. 4), an increase in the background signal was observed, which was due to an oxidisable impurity present in the substrate. When the sample is injected (at point B), the free tracer fraction (Ag*) passes through the protein G column and is detected by the GDH biosensor (peak C). Because the hydrolysis of 4-APG by the β-Gal bound inside the column is relatively slow, there is not a considerable change in the background current in the absence or presence of the As36–HOM–β-Gal complex (AbAg*) trapped inside the protein G column, (compare, for example, the current before injection (trace B) and after trapping of the antibody bound tracer (before first trace D) in Fig. 4). After the complete elimination of the Ag* fraction, the flow is stopped (at point D) for the incubation of the Ab–Ag* fraction, bound by the protein G column, with the β-Gal substrate 4-APG present in the carrier buffer. This causes an additional increase of the background current, due to the additional oxidation of the substrate impurity at the GDH biosensor (signal between traces D and E).

Even though the reaction in the column is not finished, an enzyme–substrate incubation time of 5 min was sufficient and chosen as a compromise between the signal amplitude and analysis time. When restarting the flow (at point E), the background current returns back to its original value, and the 4-AP generated during the incubation of 4-APG with the β-Gal tracer fraction trapped inside the protein G column, is detected by the GDH biosensor (peak F). This signal is inversely correlated to the analyte concentration (compare, for example the peak J, obtained in the presence of the analyte, with F, due to a sample containing only the antibody and tracer).

The apparent Michaelis constant (K_m^{app}) for the conversion of 4-APG under the action of β-Gal and direct amperometric detection of 4-AP in a similar flow system was found to be 180 μM.[26] The concentration of 4-APG necessary for exploiting the maximum β-Gal activity could not, however, be employed in the present assay. The concentration of substrate in the carrier flow was limited to only 50 μM because of the presence of an

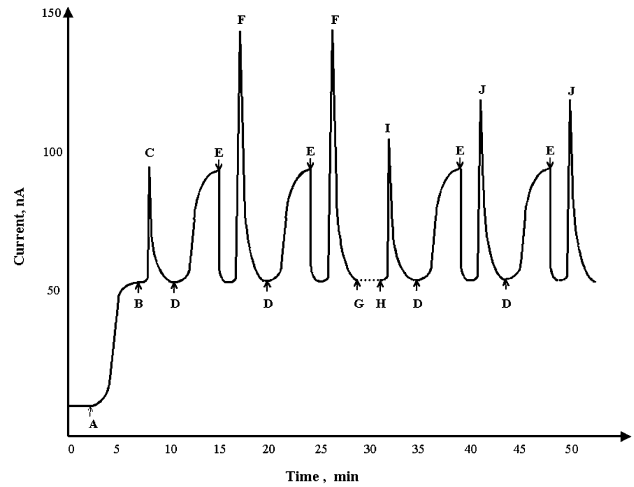

Fig. 4 Flow-injection experiments: A, the substrate 4-APG is introduced into the carrier flow where the presence of an oxidisable impurity causes an increase in the background signal; B, the reference containing only the tracer and the antibody is injected (Ab–Ag*); C and I, signals given by the tracer fraction that is not bound to the antibody (Ag*); D, stopping the flow causes a new increase in the background current; E, when the flow is restarted the background comes back to the baseline value; F, signal for the bound tracer fraction in the absence of the analyte (Ab–Ag*); G, regeneration of the protein G column; H, injection of the sample containing the analyte (Ag + Ab + Ag*); and J, the peak given by measurement of bound tracer fraction in the presence of analyte (Ab–Ag* + Ab–Ag) is recorded. The measurement of the specific signals F and J were performed in duplicate.

impurity, which at higher concentrations gave an enormous oxidation current background, (see Fig. 4, trace A→B), reducing considerably the dynamic range for the biosensor measurements.

Antibody dilution and analyte calibration. For the best assay sensitivity in competitive immunoassays the minimal possible tracer concentration has to be used. However, this decrease in concentration is limited by the deterioration in assay precision. The optimal tracer concentration was chosen in each case to be the one that gave a response about 100 times higher than the noise current, which was a signal considered sufficient for the development of an assay with a relatively good precision. None of the tracers with initial HOM to β-Gal molar ratios of 1 : 1 were recognised even at very high antibody concentrations.

Fig. 5a and 5b show the antibody dilution curves obtained for all the other tracers. As expected, the tracers synthesised from the mixture containing the highest molar ratio between the hapten and enzyme label were best recognised by the antibody, and the difference in affinity was more accentuated for the tracers synthesised by activation procedure II. Even though the same derivative, coupled to keyhole limpet hemocyanin, was used for immunisation of rabbits for production of the antisera, the apparent affinity of the antibody–tracer interaction in the EFIA was however relatively low (*i.e.*, around 10^7 M^{-1}, as seen in Table 1).

Moreover, the apparent affinity for 4-NP was even lower (*e.g.*, below 10^5 M^{-1}), so that the developed assay led to high LOD values for 4-NP (*i.e.*, in the μM range, see Fig. 6 and Table 2). The best immunoassay performances (*e.g.*, LODs around 1.5 μM) were obtained for the tracers with an intermediate hapten : enzyme label molar ratio (100 : 1), as the ideal compromise between the two effects caused by the increase in the number of HOM groups coupled to the protein structure: the decrease in the β-Gal activity (see Fig. 3) on the one hand, and the improvement of the tracer recognition by the antibody on the other (see Fig. 5 and Table 1).

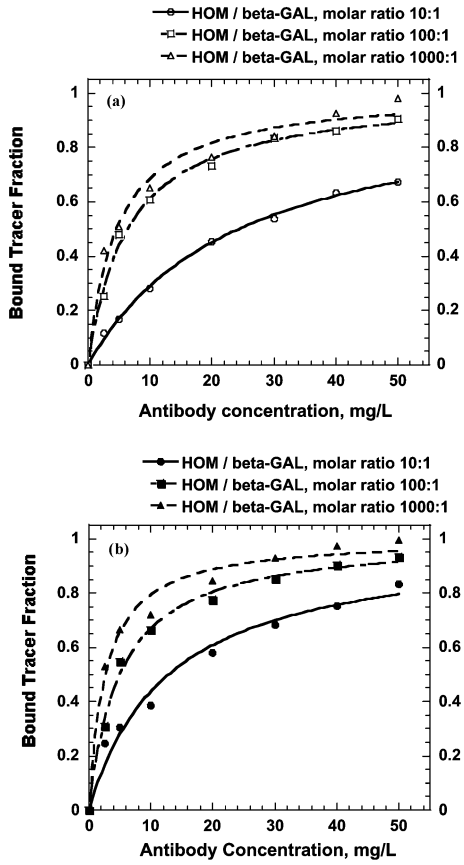

Fig. 5 Antibody dilution curves for EFIA experiments. Tracers obtained by coupling procedures I (a) and II (b). Reactant concentrations: as given in Table 2.

Microtiter plate ELISA

The results obtained with the different tracers by microtiter plate ELISA are shown in Table 3. As seen, the best tracer found for the EFIA (*e.g.*, AP II; 100 : 1) also gave the best results in the ELISA, leading to an LOD of 0.04 μM 4-NP. The reason for the better performance of the ELISA is evidently that the substrate incubation time used was 20 h as compared to 5 min in the EFIA, and also that a different substrate (*i.e.*, 4NPG) and detection mode (absorbance measurement at 405 nm) were employed, which allowed the exploitation of the full catalytic capacity of β-Gal by using a high excess of substrate. A longer substrate incubation time and higher substrate concentration allows the use of lower tracer concentrations, that in turn leads to a lower antibody consumption, thus resulting in a better LOD for the analyte.

Conclusions

This paper presents the possibility of combining an enzyme flow immunoassay (EFIA) for 4-NP with a PQQ dependent GDH biosensor as the β-Gal label detector. The EFIA method has certain benefits, as the additional amplification of the signal given by the amperometric biosensor, but also drawbacks, *i.e.* impossibility of using the optimal substrate concentration for the measurement of the enzyme label activity because of an oxidisable impurity present in the commercial substrate. The developed EFIA is compared with a microtiter plate ELISA, and the results obtained by the second technique are generally about 50 times better, but for a much longer (40 times) analysis time (30 min sample^{-1} for EFIA compared with 20 h incubation for

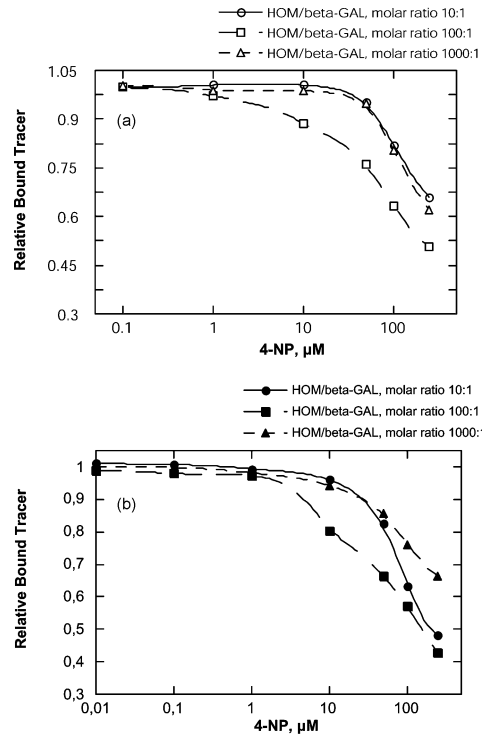

Fig. 6 4-NP calibration plots for EFIA experiments. Conditions: concentration of tracers: as in Table 1, As36 concentrations for 50% tracer binding, see Table 2. Tracers obtained by coupling procedures I (a) and II (b).

Table 2 EFIA characteristics

Tracer					
AP	HOM : β-Gal, initial molar ratio	Concentration/ nM β-Gal	$As36_{50}$[a]/mg L^{-1}	IC_{50}[b]/μM	LOD[c]/μM
I	10 : 1	1.52	12.5	90 ± 6	19.1 ± 0.9
I	100 : 1	1.05	6.5	26 ± 2	1.7 ± 0.1
I	1000 : 1	0.94	4.5	352 ± 19	15.1 ± 0.9
II	10 : 1	1.30	12.9	76 ± 5	8.54 ± 0.5
II	100 : 1	0.80	5.9	24 ± 1	1.49 ± 0.07
II	1000 : 1	0.53	2.7	259 ± 12	7.0 ± 0.3

[a] $As36_{50}$, concentration of antibody that binds 50% of the working tracer concentration. [b] IC_{50}, analyte concentration that leads to 50% inhibition of the signal in comparison with the zero dose. [c] The LOD was calculated as the concentration of analyte that led to a change in signal equal to three times the standard deviation of the signal at zero dose.

Table 3 ELISA characteristics

Tracer				
AP	HOM : β- GAL, initial molar ratio	Con- centration/ nM β-Gal	IC_{50}/μM	LOD/μM
I	10 : 1	0.012	0.28 ± 0.04	0.058 ± 0.008
I	10 : 1	0.122	0.79 ± 0.09	0.66 ± 0.08
I	10 : 1	1.215	8.1 ± 0.8	1.2 ± 0.1
I	100 : 1	0.063	2.7 ± 0.4	0.12 ± 0.02
I	100 : 1	0.629	18 ± 2	1.1 ± 0.1
I	100 : 1	6.290	72 ± 8	24 ± 3
II	10 : 1	0.036	n.d.[a]	n.d.
II	10 : 1	0.357	0.46 ± 0.06	0.055 ± 0.007
II	10 : 1	3.568	1.3 ± 0.2	0.08 ± 0.01
II	100 : 1	0.059	7.5 ± 0.9	0.040 ± 0.006
II	100 : 1	0.588	11 ± 2	0.60 ± 0.09
II	100 : 1	5.876	57 ± 5	9.4 ± 0.9

[a] n.d., not determined.

plate ELISA). The EFIA result could probably be considerable improved by a supplementary purification of the β-Gal substrate. This was verified in a later work when a different batch of 4-APG from the same source allowed the use of a higher substrate concentration in an assay configuration based on immobilised antibodies, so that the β-Gal activity could be more efficiently exploited. An improvement in EFIA performances can also be expected by the increase of incubation time between the 4-APG substrate and the β-Gal fraction trapped inside the protein G-based column.

Acknowledgements

The authors kindly acknowledge financial support from the European Community (EC no. ENV4-CT97-0476, IC15-CT98-0119 and IC15-CT98-0138), the Swedish Foundation for Strategic Environmental Research (MISTRA), the Swedish Council for Forestry and Agricultural Research (SJFR), the Swedish Research Council (Vetenskapsrådet), and the Swedish Environmental Protection Agency (NVV-Naturvårdsverket). The authors are grateful to Dr A. Makower for valuable discussions and to Dr M-P. Marco for providing the immunoreagent.

References

1 Y. Ding, L. Zhou, H. B. Halsall and W. R. Heinemann, *J. Pharm. Biomed. Anal.*, 1999, **19**, 153–161.
2 H. T. Tang, C. E. Lunte, H. B. Halsall and W. R. Heinemann, *Anal. Chim. Acta*, 1988, **214**, 187–195.
3 Y. Xu, H. B. Halsall and W. R. Heinemann, *J. Pharm. Biomed. Anal.*, 1989, **7**, 1301–1311.
4 O. Niwa, Y. Xu, H. B. Halsall and W. R. Heinemann, *Anal. Chem.*, 1993, **65**, 1559–1563.
5 F. F. Bier, E. Ehrentreich-Förster, C. G. Bauer and F. W. Scheller, *Fresenius' J. Anal. Chem.*, 1996, **354**, 861–865.
6 H. Gao, T. Jiang, W. R. Heineman, H. B. Halsall and J. L. Caruso, *Fresenius' J. Anal. Chem.*, 1999, **364**, 170–174.
7 C. A. Wijayawardhana, H. B. Halsall and W. R. Heineman, *Anal. Chim. Acta*, 1999, **399**, 3–11.
8 A. E. G. Cass, W. J. Albery and A. R. Hopkins, *PCT Int. Appl.*, 8702464, 1987, 25 pp.
9 M. Del Carlo and M. Mascini, *Anal. Chim. Acta*, 1996, **336**, 167–174.
10 S. Zhang, K. Jiao, H. Chen and M. Wang, *Talanta*, 1999, **50**, 95–101.
11 K. Jiao, W. Sun, S.-S. Zhang and G. Sun, *Anal. Chim. Acta*, 2000, **413**, 71–78.
12 W. Sun, K. Jiao and S.-S. Zhang, *Anal. Lett.*, 2000, **33**, 2653–2675.
13 W. Sun, K. Jiao, S.-S. Zhang, C. Zhang and Z. Zhang, *Anal. Chim. Acta*, 2001, **434**, 43–50.
14 M. E. Brown, L. S. Kuhn, R. J. McEnroe, R. W. Muddiman, M. L. Ochs, J. G. R. Hurrell and H. J. Guder, *PCT Int. Appl.*, 9506115, 1995, 35 pp.
15 R. D. Macphee, C. R. Taylor, R. Hintsche and R. Seitz, *PCT Int. Appl.*, 9907879, 1999, 44 pp.
16 E. Burestedt, C. Nistor, U. Schagerlöf and J. Emneús, *Anal. Chem.*, 2000, **72**, 4171–4177.
17 W. O. Ho, D. Athey and C. J. McNeil, *Biosens. Bioelectron.*, 1995, **10**, 683–91.
18 C. G. Bauer, A. V. Eremenko, E. Ehrentreich-Förster, F. F. Bier, A. Makower, B. H. Halsall, W. R. Heineman and F. W. Scheller, *Anal. Chem.*, 1996, **68**, 2453–2458.
19 C. G. Bauer, A. V. Eremenko, A. Kuhn, K. Kürzinger, A. Makower and F. W. Scheller, *Anal. Chem.*, 1998, **70**, 4624–4630.
20 C. Nistor and J. Emnéus, *Anal. Commun.*, 1998, **35**, 417–419.
21 C. Nistor, A. Osvik, R. Davidsson, A. Rose, U. Wollenberger, D. Pfeiffer, J. Emnéus and L. Fiksdal, *Water Sci. Technol.*, 2002, **45**, 191–199.
22 A. Rose, F. Scheller, U. Wollenberger and D. Pfeiffer, *Fresenius' J. Anal. Chem.*, 2001, **369**, 145–152.
23 M. M. Bradford, *Anal. Biochem.*, 1976, **72**, 248–254.
24 C. Nistor, M. Tudorache, M.-P. Marco and J. Emnéus, unpublished results, 2002.
25 C. Davies, in *The Immunoassay Handbook*, ed. D. Wild, Stockton Press, New York, 1994, pp. 8–38.
26 A. Rose, C. Nistor, J. Emnéus, D. Pfeiffer and U. Wollenberger, *Biosens. Bioelectron.*, 2002, in press.